



Cite this: *React. Chem. Eng.*, 2023, **8**, 2826

## Optimized design and techno-economic analysis of novel DME production processes†

Malte Semmel, <sup>ab</sup> Maximilian Kerschbaum,<sup>a</sup> Benedikt Steinbach,<sup>a</sup> Jörg Sauer <sup>b</sup> and Ouda Salem <sup>\*a</sup>

The shift from gas to liquid phase DME synthesis enables an intensified process concept towards efficient large scale DME production. In this work, four process concepts based on liquid phase DME synthesis were proposed and optimized. A comprehensive economic model was applied with the objective of minimizing the total production cost. All concepts were evaluated applying our previously validated reaction kinetics for commercial ion exchange resin selected catalysts. Furthermore, every process concept was studied with a pure MeOH feed and water-rich (crude) MeOH feedstock. The conventional gas-phase DME production process was simulated and evaluated using the same technical and economic parameters to serve as a benchmark. Using a chlorinated high temperature stable IER catalyst led to significant cost reduction in all the considered concepts. This was due to the higher reaction rate enabled by the higher operating temperature of this catalyst. In the integrated process concept with H<sub>2</sub> and CO<sub>2</sub> as sustainable feedstocks, it was shown that the reactive distillation process shows a 27% lower production cost, when the crude methanol is directly fed to the DME process instead of being purified in a dedicated crude methanol distillation column. A further techno-economic optimization can be achieved when complementing the reactive distillation column with an additional reactor. Overall, the process concept of a reactive distillation column with a side reactor presents the most promising process concept, enabling a 39% lower production cost than the conventional gas-phase process. By heat integration with a CO<sub>2</sub>-based MeOH plant, a DME production technology with no external heat demand and a net conversion cost of 54.4 € per t<sub>DME</sub> is possible.

Received 16th June 2023,  
Accepted 18th July 2023

DOI: 10.1039/d3re00333g

rsc.li/reaction-engineering

## Introduction

Hydrogen is a key element for the defossilisation of the energy economy.<sup>1,2</sup> A large share of the hydrogen demand will be in industrial countries with limited potential for renewable energy generation, while economically attractive green hydrogen production is allocated at regions with high abundance of renewable energy resources. A promising strategy to solve this mismatch and to integrate the renewable energy potential from countries of the global south into the energy system of industrial countries lies in the efficient transport of hydrogen and its derivatives. Current forecasts predict a global hydrogen production capacity of 24<sup>3</sup>–38<sup>4</sup> Mtpa by 2030 of which around 12 Mt of hydrogen will be traded.<sup>3</sup>

Dimethyl ether (DME, CH<sub>3</sub>–O–CH<sub>3</sub>) is an excellent hydrogen carrier with 26 wt% technical H<sub>2</sub> capacity (48% higher storage capacity than ammonia), environmentally benign properties and similar physiochemical properties to CO<sub>2</sub>. This could allow the establishment of a closed DME/CO<sub>2</sub> cycle for sustainable global H<sub>2</sub> transport at a large scale.<sup>5</sup> With existing global production capacities of about 10 Mtpa, DME is an important methanol derivative. The major current use of DME is in blending with LPG. This sector demand alone is projected to reach an annual DME production of 40 Mt by 2050, a fourfold increase compared to the current global production capacities.<sup>6,7</sup>

Conventionally, DME is produced *via* the equilibrium-limited dehydration of pure MeOH in the gas phase and consecutive two-step distillation of the ternary MeOH–DME–H<sub>2</sub>O product mixture. Besides being a rather complex plant layout, this process implies a high energy demand, since the MeOH feedstock needs to be evaporated and heated up to the elevated DME reaction temperature above 275 °C.<sup>8</sup> Furthermore, the conventional catalytic process is not capable of converting water-rich crude MeOH, thus requiring the purification of MeOH in a dedicated crude MeOH

<sup>a</sup> Fraunhofer Institute for Solar Energy Systems ISE, Heidenhofstr. 2, 79110 Freiburg, Germany. E-mail: [ouda.salem@ise.fraunhofer.de](mailto:ouda.salem@ise.fraunhofer.de)

<sup>b</sup> Karlsruhe Institute of Technology (KIT), Hermann-von-Helmholtz-Platz 1, D-76344 Eggenstein-Leopoldshafen, Germany

† Electronic supplementary information (ESI) available. See DOI: <https://doi.org/10.1039/d3re00333g>



distillation column prior to the conversion to DME. An alternative process is the direct synthesis of DME from syngas. While the coupling of MeOH and DME synthesis entails the advantage of an increased CO<sub>2</sub> conversion, the downstream processing in this process is more complex as the presence of DME in the reactor product hampers the separation and recycling of syngas. Furthermore, for CO<sub>2</sub>-rich syngas, the process is thermodynamically inhibited due to strong water production.<sup>9,10</sup>

Liquid phase DME synthesis presents a promising technological alternative since it allows the omission of the methanol (MeOH) evaporation step and thus can reduce the energy demand and the investment cost of the process. Furthermore, the liquid phase synthesis enables the application of a reactive distillation process that on the one hand has the potential to significantly reduce plant complexity and the investment cost, and on the other hand allows the feed of crude MeOH, since the reaction occurs in an apparatus with *in situ* water removal.

In a previous study of our group, promising catalysts for the liquid phase DME synthesis were screened, and a kinetic model was derived for the two ion exchange resin (IER) catalysts Amberlyst 36 (A36) and Treverlyst CAT 400 (C400).<sup>11</sup> The reaction kinetics on the chlorinated IER C400 was reported to allow significantly higher reaction rates compared to the oversulfonated IER A36 due to the higher thermal stability of the catalyst.

In another recent publication,<sup>12</sup> a reactive distillation process producing purified DME from pure and crude MeOH feed was demonstrated experimentally and a validated process simulation model was derived. Thereby, all existing kinetic models in the literature for liquid phase DME synthesis were evaluated with RDC experiments under industrially relevant conditions and it was shown that only the kinetic model by Semmel *et al.*<sup>11</sup> precisely describes the reaction kinetics. Additionally, it was shown that the reactive distillation process entails a distinct target conflict between the energy demand and column size. A realistic evaluation of the process thus requires a total cost optimized design of the reactive distillation column (RDC) based on a techno-economic analysis.

A process optimization minimizing total production cost has been performed in the literature by Bildea *et al.*<sup>8</sup> for a RDC using a pure MeOH feedstock and employing the kinetic model by Hosseinijad *et al.*<sup>13</sup> Gor *et al.*<sup>14</sup> did a total production cost optimized design of a reactive distillation and reactive dividing wall column, employing the kinetic model by Lei *et al.*<sup>15</sup> Wu *et al.*<sup>16</sup> examined two RD configurations, also employing the kinetic model by Lei *et al.*<sup>15</sup> and optimized them with regard to minimum CO<sub>2</sub> emission. All previous public literature is based on oversulfonated IER, with a maximum operating temperature of 150 °C according to the manufacturer.

In the scope of this work, various process concepts based on the liquid-phase DME synthesis and the corresponding thermal or reactive separation are proposed. The main

objective is to identify the process concept allowing the lowest conversion cost of MeOH to DME with the highest energy efficiency. To allow a fair comparison, each process concept is optimized on its own with the objective of identifying the optimum configuration in terms of minimum production cost. Besides using only pure MeOH feed and an oversulfonated IER catalyst as described in the literature, all process concepts are also evaluated for crude MeOH feed and for chlorinated IER catalysts. Finally, all processes are compared with each other and finally with the conventional process as a benchmark. The process with the lowest production cost is further considered for a detailed energy integration with the MeOH synthesis starting from CO<sub>2</sub> and H<sub>2</sub> feedstocks.

## Process overview and system boundaries

In total, 5 process concepts were evaluated in this work as summarized in Fig. 1. Process P0 presents the conventional gas-phase DME process, consisting of a feed evaporator, a gas phase reactor converting MeOH *via* dehydration to DME and H<sub>2</sub>O, and two distillation columns with MeOH recycling. In comparison, process P1 also consists of a reactor-separation-recycling configuration. However, the reactor is operated in the liquid phase and consequently no evaporation step is required. Process P2 is the intensified process alternative based on a stand-alone RDC. While the advantages of this process have already been discussed, the RDC entails particularly two challenges: on the one hand, the RDC exhibits a system inherent temperature profile across the reactive section. This prevents conducting the reaction at the optimal temperature level in the entire reactive section, thus demanding a large amount of catalyst in the RDC. On the other hand, the insertion of the catalyst into a distillation column requires relatively expensive column internals such as catalytic packings. These two challenges can potentially be overcome by the integration of a fixed-bed reactor into the process, in which a partial reaction conversion can be achieved. While this additional reactor is limited by the thermodynamic equilibrium, it allows the reaction to be carried out isothermally at the optimal reaction temperature and without the need for expensive internals. Two possible allocations of this strategy are process P3, complementing the RDC with a pre-reactor (PR), and process P4, adding a side-reactor (SR) to the RDC. In both processes, the reactor product is forwarded to a flash in order to obtain a DME-rich phase and a water-rich phase. Both streams are fed to the RDC on separate stages.

The reference feedstock for the process is pure methanol. For comparison, crude MeOH feed is considered, consisting of 50 mol% water and 50 mol% MeOH at a temperature of 25 °C. The composition was chosen following Nyári *et al.*<sup>17</sup> and presented a typical composition for a CO<sub>2</sub>-based MeOH synthesis process. For all the novel process concepts, two cases are distinguished: in the first case, water is removed







uncorrected version of the kinetic model consequently obtained significant deviations in the reaction rate.

### Reactive distillation column

The RDC is simulated using an equilibrium-based separation approach based on the RADFRAC model, which assumes the liquid and gas phases of each stage to be ideally mixed. On the catalyst containing reactive stages in the middle of the column, the reaction is modelled using the kinetics by Semmel *et al.*<sup>11</sup> implemented with a Fortran subroutine. The top and bottom sections of the column do not contain a catalyst and are modelled as rectifying stages only. The upper rectifying section includes 10 theoretical stages, and the lower rectifying section includes 15 theoretical stages. The reactive section was implemented with 40 theoretical stages.

The operating pressure of the RDC is varied by a design specification so that the maximum temperature in the reactive section is equal to the maximum operating temperature of the used catalyst. A second design specification modifies the RR so that the DME purity equals 99.9 mol% under full MeOH conversion. Details regarding the RDC modelling and the thermodynamic property calculation can be found in Semmel *et al.*<sup>12</sup>

The weight hourly space velocity (WHSV) of the RDC is defined as follows:

$$\text{WHSV} = \frac{\dot{m}_{\text{Feed, MeOH}}}{m_{\text{catalyst, RDC}}} \quad (1)$$

The catalyst is assumed to be introduced into the column using catalytic packing internals such as KATAPAK®. Catalytic packing internals are available with different distributions between catalyst bags and corrugated wire gauze sheets. In a previous study, it was shown that DME RD is a kinetically limited process and consequently, at a constant catalyst mass, the number of stages in the reactive section has a negligible influence on the process.<sup>12</sup> As a result, a catalytic packing design with maximum catalyst capacity should be employed for DME synthesis. The catalyst volume fraction of this packing type  $\psi_{\text{cp}}$  (volume of the catalyst bulk divided by the packing volume) at the industrial scale is typically 0.55 according to Hoffmann *et al.*<sup>24</sup> Consequently, the volume of the reactive section can be calculated from the required catalyst mass according to the following equation:

$$V_{\text{reactive section}} = \frac{m_{\text{cat}}}{\rho_{\text{cat, bulk}} \cdot \psi_{\text{cp}}} \quad (2)$$

The rectifying sections are equipped with conventional structured packing (Mellapak) with a HETP of 0.5 m.<sup>25</sup>

### Distillation columns

The distillation columns in all the processes are modelled using the RADFRAC standard equilibrium-based model in

Aspen Plus. Structured packings (Mellapak) with a HETP of 0.5 m (ref. 25) were selected as column internals. The column diameter was calculated with the Aspen internal hydraulics tool.

### Economic model

Economic evaluation of each process was done based on the factorial method approach. A detailed description of the methodology is described by Albrecht *et al.*<sup>18</sup> According to AACE (Association for the Advancement of Cost Engineering) classes three and four, an accuracy of  $\pm 30\%$  can be expected based on this methodology.<sup>26</sup> The year 2020 was chosen as the base year. The used economic assumptions are summarized in Table 2.

The overall production costs are composed of the CAPEX and OPEX of the plant.

### CAPEX

CAPEX is calculated as fixed capital investment (FCI) based on the equipment cost  $EC_i$  of the main process equipment and Lang factors  $F_i$ . Annualized capital cost (ACC) is then derived from FCI using the interest rate  $i$ , working capital share  $w$  and the plant operation time  $n$  according to eqn (3) and (4). The Lang factors are summarized in the ESI.†

$$\text{FCI} = (1 + F_{\text{Contractor}} + F_{\text{Contingency}}) \cdot \quad (3)$$

$$\left( 1 + \sum_j F_{\text{dir},j} + \sum_k F_{\text{ind},k} \right) \cdot \sum_i EC_i$$

$$\text{ACC} = \text{FCI} \cdot \left( \frac{i \cdot (1+i)^n}{(1+i)^n - 1} + \frac{w}{1-w} \cdot i \cdot n \right) \quad (4)$$

The equipment cost is calculated by regressed cost functions based on the published cost data by Peters *et al.*<sup>29</sup> Each cost function is scaled with all relevant sizing parameters of the respective apparatus to account for the economy of scale. Additional costs due to pressure stability are accounted for by a dedicated pressure correction function. All cost functions and the

**Table 2** Economic parameters and assumptions

| Parameter                 | Unit                                     | Value           |
|---------------------------|--|-----------------|
| Plant capacity            | $\tau_{\text{DME}}$ per year             | 100 600         |
| Plant availability        | h per year                               | 8000            |
| Location                  | —  | Germany         |
| Base year                 | —  | 2020            |
| Project lifetime $n$      | Year                                     | 20              |
| Interest rate $i$         | %  | 5 (ref. 20)     |
| Working capital share $w$ | —  | 0.1 (ref. 18)   |
| Exchange rate             | € <sub>2020</sub> per \$ <sub>2020</sub> | 0.876 (ref. 27) |
| Labor cost                | € per h                                  | 41.0 (ref. 28)  |







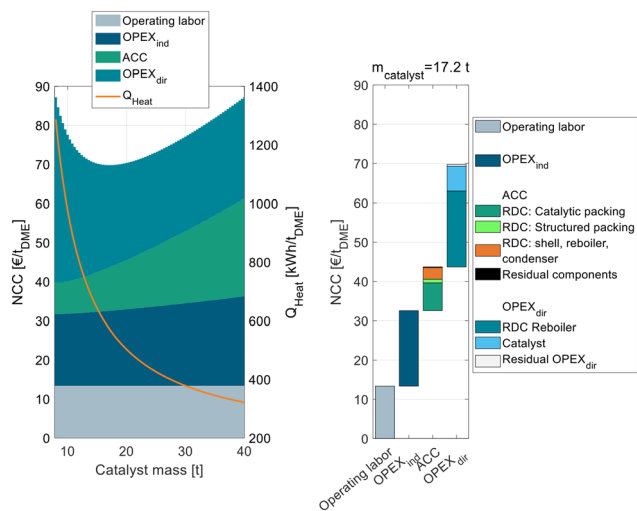


**Fig. 4** Heat demand and NCC of the RD process P2 with C400 and pure MeOH feed in dependence of the catalyst mass in the RDC broken down into ACC, OPEX<sub>ind</sub>, and OPEX<sub>dir</sub> (left) as well as detailed cost breakdown at the cost optimum (right).

the optimal feed stage. Table 6 shows the KPIs of the final optimized configuration.

To analyze this process in more detail, Fig. 4 shows exemplarily for C400 and pure MeOH feed the NCC of process P2 broken down into ACC, OPEX<sub>ind</sub> and OPEX<sub>dir</sub> and operating labor on the left side.

The figure shows the RDC-inherent target conflict between capital expenses and operating expenses: while a small RDC with little catalyst mass leads to a low ACC, a high RR and consequently a high energy demand are required to achieve the desired full MeOH conversion in the RDC. Increasing the catalyst mass of the RDC increases the ACC, since the column size and the amount of catalytic packing increase but reduce the RR and OPEX<sub>dir</sub> so that an optimum catalyst mass of 17.2 t can be identified. The corresponding WHSV is 1.02 h<sup>-1</sup>. The exact position of the minimum depends on all assumptions influencing the ACC or OPEX. While only one cost optimal RDC size exists, this optimum is rather “flat”. Consequently, the RDC size and the resulting energy demand of the process can be designed in a wide range without the NCC deviating significantly from the optimal configuration. Also, in the case of temporally reduced feed availability, the plant can be operated at lower WHSV which will reduce the specific energy demand of the plant.

Compared to the conventional process P0, the RD process is characterized by a higher ACC which can majorly be attributed to the higher required catalyst mass due to the significantly lower reaction temperature. The OPEX<sub>dir</sub> is comparable for both processes: while the RD process P2 has a lower steam cost due to a lower energy demand (569 kW h t<sub>DME</sub><sup>-1</sup> vs. 762 kW h t<sub>DME</sub><sup>-1</sup>), this benefit is compensated by the significantly higher catalyst cost to the higher catalyst mass and the lower assumed catalyst lifetime of IER compared to  $\gamma$ -Al<sub>2</sub>O<sub>3</sub>. The right side of Fig. 4 shows the detailed cost breakdown at the optimum catalyst mass. The ACC is dominated by the RDC, particularly

the cost of the catalytic packing internals and the cost for the RDC shell, reboiler and condenser. In contrast, the cost for the other process components (pump, heat exchangers) and the structured packing in the RDC is almost negligible. The OPEX<sub>dir</sub> is dominated by the heat demand of the RDC reboiler, but the influence of the catalyst cost is also significant.

In comparison with C400, process P2 with A36 shows its optimum at a significantly higher catalyst mass of 40.8 t. Nevertheless, the required RR is higher than that for C400, again underlying the great benefit of the higher reaction rate through higher temperature stability. As a consequence, C400 is able to reduce both the RDC size and the energy demand compared to A36.

For crude MeOH, the optimal feed stage moves down to the bottom of the reactive section, where the water-containing crude MeOH better fits the column profile. As another consequence of the crude MeOH feed, the energy demand and the required catalyst mass are higher as the reaction kinetics is hampered by the higher water content of the feed and more water needs to be evaporated in the reboiler in total. Also, for crude MeOH C400 shows significant improvements compared to A36 regarding the energy demand and NCC. Interestingly, even C400 with crude MeOH feed leads to a lower NCC than A36 with pure MeOH feed.

**P3: RDC with a pre-reactor.** Process P3 adds significant complexity compared to P2, as the reactor product from the PR performs flash separation and consequently 2 feed stages need to be optimized. Table 7 shows the optimized parameters and KPIs. For both feeds and catalysts, the configuration is very similar with the feed stage of the DME-rich phase being in the upper rectifying section and that of the H<sub>2</sub>O-rich phase in the lower rectifying section or the last stage of the reactive section (A36 with pure MeOH feed).

Besides the two feed stages, the optimal size needs to be determined for the PR and RDC. While a larger PR leads to increased cost for the reactor, the increased MeOH conversion allows the RDC to be smaller or operate at a lower RR. Consequently, a target conflict between the PR size and RDC size is present in the system.

Fig. 5 shows this interplay between the PR and RDC sizes. For each RDC size an optimal PR size can be identified. With increasing RDC size, the optimal PR size decreases, the best

**Table 7** KPIs at the optimized process configuration of process P3 for pure and crude MeOH feed and both catalysts

| Parameter                          | Unit                                | Pure MeOH |      | Crude MeOH |      |
|------------------------------------|-------------------------------------|-----------|------|------------|------|
|                                    |                                     | A36       | C400 | A36        | C400 |
| $N_{\text{Feed,DME-rich}}$         | —                                   | 7         | 9    | 9          | 7    |
| $N_{\text{Feed,H}_2\text{O-rich}}$ | —                                   | 50        | 56   | 56         | 54   |
| $m_{\text{Cat,PR}}$                | t                                   | 10.8      | 8.4  | 8.2        | 11.1 |
| $X_{\text{MeOH,PR}}$               | —                                   | 0.52      | 0.91 | 0.09       | 0.52 |
| $m_{\text{Cat,RDC}}$               | t                                   | 23.0      | 1.6  | 40.0       | 9.2  |
| RR                                 | —                                   | 5.7       | 0.8  | 13.1       | 6.2  |
| $Q_{\text{Heat}}$                  | kW h t <sub>DME</sub> <sup>-1</sup> | 756       | 238  | 1530       | 783  |
| NCC                                | € per t <sub>DME</sub>              | 88.9      | 52.4 | 129.5      | 85.5 |











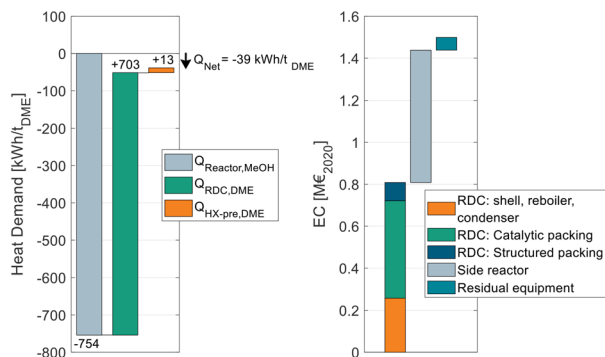


**Fig. 9** Energy demand of process P4 when heat integrated with the reactor of a MeOH synthesis plant (left) and equipment cost breakdown of the DME process (right).

On the left side of the diagram, the exothermic heat of the MeOH reactor is displayed as a negative energy demand. Consequently, it is offset against the two energy demanding apparatuses of the DME process, namely the RDC and the SR feed heat exchanger HX-pre. From the illustration, a net heat demand of  $Q_{\text{Net}} = -39 \text{ kW h } t_{\text{DME}}^{-1}$  at the MeOH reaction temperature can be identified, implying that the integrated process releases more heat than it consumes. The only energy demand of the DME process is the electric energy required for the pumps P-Feed and P-SR which is  $11.4 \text{ kW h}_{\text{el}} t_{\text{DME}}^{-1}$ . The MeOH synthesis plant has no external heat demand either, as a feed to product heat exchanger is sufficient to heat up the feed gas. Overall, process P4 allows a DME production process from  $\text{CO}_2$  and  $\text{H}_2$  feedstocks with no external heat demand. Instead, the process entails the possibility of exporting 39 kW h of MP steam per ton of DME produced. This is a decisive advantage in the PtX context, where plants are more likely to be constructed in remote areas without the infrastructure commonly found in chemistry parks. Integrating the “free” heat from the MeOH synthesis reduces the NCC of the process from 79.6 € per  $t_{\text{DME}}$  (no heat integration, Table 8) to 55.6 € per  $t_{\text{DME}}$  as the steam costs can be omitted. As the amount of exothermic heat is even higher than the heat demand, in this process configuration, the residual excess heat of  $39 \text{ kW h } t_{\text{DME}}^{-1}$

**Table 9** KPIs of process P4 for crude MeOH feed and C400 at the optimized process configuration when heat integrated with a MeOH plant

| Parameter                         | Unit                               | Crude MeOH |
|-----------------------------------|------------------------------------|------------|
|                                   |                                    | C400       |
| $N_{\text{Feed}}$                 | —                                  | 15         |
| $N_{\text{WD}}$                   | —                                  | 9          |
| $N_{\text{RCY,DME-rich}}$         | —                                  | 7          |
| $N_{\text{RCY,H}_2\text{O-rich}}$ | —                                  | 56         |
| Sidestream                        | $\text{kmol h}^{-1}$               | 525        |
| $m_{\text{Cat,SR}}$               | t                                  | 8.9        |
| $X_{\text{MeOH,SR}}$              | —                                  | 0.87       |
| $m_{\text{Cat,RDC}}$              | t                                  | 8.8        |
| RR                                | —                                  | 5.9        |
| $Q_{\text{Heat}}$                 | $\text{kW h } t_{\text{DME}}^{-1}$ | 0          |
| NCC                               | € per $t_{\text{DME}}$             | 54.4       |



**Fig. 10** NPC of DME in dependence of the crude MeOH feedstock cost, as calculated by eqn (7). Cost for the optimal process presented in this work and comparison with the theoretical minimal cost, when neglecting all cost for the DME process.

would be dissipated. Consequently, by reoptimizing the process under the boundary conditions of using the entire available exothermic heat, a new optimal configuration can be found that is characterized by a higher reboiler duty of the RDC but lower CAPEX. Table 9 sums up the KPIs at this process design configuration.

### Calculation of the NPC

All results presented to this point reflect the NCC, considering all cost related to the DME synthesis itself, but disregarding the cost for the MeOH feedstock. Since the crude MeOH cost is dependent on many factors, Fig. 10 shows the NPC of DME produced *via* P4 with C400 and crude MeOH feed as a function of the crude MeOH cost. The process design configuration of P4 was chosen as shown in Table 9. For comparison, the theoretical minimum NPC is shown. In this case, the OPEX and CAPEX for the DME process are neglected and only the feedstock cost is considered.

The NPC increases linearly with the crude MeOH cost, thereby reflecting the linear character of eqn (7). The NCC of the DME process is visible as the vertical distance between the two lines in the diagram.

## Conclusions and outlook

DME shows very promising properties for global transport of green hydrogen. Shifting the reaction phase of DME synthesis from gas to liquid opens up new possibilities towards the design of novel efficient process concepts. In the scope of this work, four process concepts were proposed and rigorously optimized with respect to the ideal process configuration and the ideal size of the RDC and/or reactor. The used process simulation platform was validated in







- [separation-technology/distillation-and-absorption/brochures/structured\\_packings.ashx](#).
- 26 Association for the Advancement of Cost Engineering (AACE), *18R-97: Cost Estimate Classification System – As Applied in Engineering, Procurement, and Construction for the Process Industries*, [https://web.aacei.org/docs/default-source/toc/toc\\_18r-97.pdf?sfvrsn=4](https://web.aacei.org/docs/default-source/toc/toc_18r-97.pdf?sfvrsn=4), (accessed 11 July 2023).
- 27 Euro-Referenzkurse, [https://www.ecb.europa.eu/stats/policy\\_and\\_exchange\\_rates/euro\\_reference\\_exchange\\_rates/html/eurofxref-graph-usd.de.html](https://www.ecb.europa.eu/stats/policy_and_exchange_rates/euro_reference_exchange_rates/html/eurofxref-graph-usd.de.html), (accessed 17 March 2023).
- 28 *Arbeitskosten in der EU, 2018*, <https://ec.europa.eu/eurostat/documents/2995521/8791193/3-09042018-BP-DE.pdf/bcad2022-0fbc-4c21-811d-5fef8399ee5f>, (accessed 1 March 2023).
- 29 M. S. Peters, K. D. Timmerhaus and R. E. West, *Plant design and economics for chemical engineers*, McGraw-Hill, Boston, 5th edn, 2003.
- 30 S. Michailos, S. McCord, V. Sick, G. Stokes and P. Styring, Dimethyl ether synthesis via captured CO<sub>2</sub> hydrogenation within the power to liquids concept: A techno-economic assessment, *Energy Convers. Manag.*, 2019, **184**, 262–276.
- 31 R. Taylor and R. Krishna, Modelling reactive distillation, *Chem. Eng. Sci.*, 2000, **55**, 5183–5229.
- 32 T. Keller, in *Distillation*, Elsevier, 2014, pp. 261–294.

